BIOCHEMISTRY
including biophysical chemistry & molecular biology
Article

Biochemistry **2010,** *49,* 7303–7313 7303
DOI: 10.1021/bi101001v

Ca^{2+} Sensor GCAP1: A Constitutive Element of the ONE-GC-Modulated Odorant Signal Transduction Pathway†

Alexandre Pertzev,‡ Teresa Duda,*,‡ and Rameshwar K. Sharma*

Research Divisions of Biochemistry and Molecular Biology, The Unit of Regulatory and Molecular Biology, Salus University, Elkins Park, Pennsylvania 19027 ‡These authors contributed equally to this work.

Received June 21, 2010; Revised Manuscript Received July 12, 2010

ABSTRACT: In a small subset of the olfactory sensory neurons, the odorant receptor ONE-GC guanylate cyclase is a central transduction component of the cyclic GMP signaling pathway. In a two-step transduction model, the odorant, uroguanylin, binds to the extracellular domain and activates its intracellular domain to generate the odorant second messenger, cyclic GMP. This study via comprehensive technology, including gene deletion, live cell Förster resonance energy transfer (FRET), and surface plasmon resonance (SPR) spectroscopy, documents the identity of a remarkably intriguing operation of a Ca^{2+} sensor component of the ONE-GC transduction machinery, GCAP1. In the ciliary membranes, the sites of odorant transduction, GCAP1 is biochemically and physiologically coupled to ONE-GC. Strikingly, this coupling reverses its well-established function in ROS-GC1 signaling, linked with phototransduction. In response to the free Ca^{2+} range from nanomolar to semimicromolar, it inhibits ROS-GC1, yet in this range, it incrementally stimulates ONE-GC. These two opposite modes of signaling two SENSORY processes by a single Ca^{2+} sensor define a new transduction paradigm of membrane guanylate cyclases. This paradigm is pictorially presented.

The odorant signal is initiated at the ciliated apical border of the olfactory sensory neurons located in the main olfactory epithelium (MOE). Binding of an odorant to its receptor generates an electrical signal. The biochemical term for this process is odorant transduction (reviewed in refs (*1*−*4*)). It is a two-step process; in the first step, the signal generates its second messenger, and in the second step, the second messenger transforms the signal into an electrical signal, which then becomes a means of signal transmission and the final perception of smell in the cortical layers of the brain.

Until recently, the only second messenger of the odorant signal was considered to be cyclic AMP (*5*−*9*). Although it still remains the major messenger, it is not the sole second messenger.

In the incremental development of the field, it has now been established that cyclic GMP is also the second messenger of the odorant signal (*10*−*14*) (reviewed in refs *1* and *15*−*17*; also see ref *18* for recent discussion). This signaling pathway resides in a small population of the olfactory receptor neurons (ORN) and is independent of the cyclic AMP signaling pathway (*11*, *12*). The pathway begins with the ONE-GC[1] membrane guanylate cyclase [also named GC-D (*10*)], which is copresent with the specific cyclic GMP-dependent components, cyclic GMP-specific cyclic nucleotide-gated channel subunit, CNGA3, and a cyclic GMP-dependent phosphodiesterase, PDE2 (*11*, *12*).

Importantly, the *modi operandi* of these two odorant pathways are radically different. In contrast to the cyclic AMP pathway, the cyclic GMP pathway does not function through the GTP-binding protein, G_{olf}. It originates from ONE-GC, which is both the receptor for the odorants uroguanylin (*19*, *20*) and green pepper (*14*, *21*) and the transducer through its guanylate cyclase activity. Thus, in line with the prototype ANF-RGC membrane guanylate cyclase signal transduction model (*22*), the coexistence of the uroguanylin receptor and guanylate cyclase activities on a single transmembrane-spanning polypeptide chain makes the cyclic GMP signal transduction pathway more direct and, theoretically, faster.

Among the multiple membrane guanylate cyclase signal transduction mechanisms, the odorant-linked ONE-GC mechanism is unique in several aspects (reviewed in ref *17*). It does not fit into the two traditional transduction models represented by the two membrane guanylate cyclase subfamilies. Unlike the Ca^{2+}-modulated ROS-GC subfamily, it recognizes the signal through its extracellular domain, and unlike the hormone receptor subfamily but like the ROS-GC subfamily, the odorant signal after its transmission to the intracellular domain undergoes multiple Ca^{2+}-modulated steps. These steps amplify the signal prior to its final translation at the catalytic site into the production of cyclic GMP, the odorant's second messenger.

ONE-GC in addition to being an odorant receptor and transducer possesses an additional intriguing feature. Indirectly, through a carbonic anhydrase enzyme, its catalytic site senses atmospheric CO_2 and accelerates the production of cyclic GMP (*23*, *24*). For these reasons, ONE-GC represents the third subfamily of membrane guanylate cyclases, which accounts for the hybrid features of the other two subfamilies: peptide hormone receptor and Ca^{2+}-modulated ROS-GC (*18*, *20*).

†This study was supported by National Institutes of Health Grants HL084584 and HL084584S.

*To whom correspondence should be addressed. R.K.S.: e-mail, rsharma@salus.edu; phone, (215) 780-3124; fax, (215) 780-3125. T.D.: e-mail, tduda@salus.edu; phone, (215) 780-3112; fax, (215) 780-3125.

[1]Abbreviations: ANF-RGC, atrial natriuretic factor receptor guanylate cyclase; FRET, Förster resonance energy transfer; GCAP, guanylate cyclase activating protein; ONE-GC, olfactory neuroepithelial guanylate cyclase; ROS-GC, rod outer segment guanylate cyclase.

Published on Web 07/27/2010

In the current odorant, uroguanylin, two-step model, in step one, the odorant binds ONE-GC and primes it for stimulation, causing its partial activation. This step is Ca^{2+}-independent (*25*). In step two, Ca^{2+}-bound neurocalcin δ through a defined intracellular domain saturates ONE-GC activity and depolarizes the ciliary membranes (*25*).

Besides neurocalcin δ, two other Ca^{2+} sensors coexist with ONE-GC. They are hippocalcin (*26*) and GCAP1 (*27*). However, the applicability of the two-step model for these signal transducers has not been studied. This study investigates the role of GCAP1, at the biochemical and physiological level, in odorant ONE-GC signal transduction. The findings demonstrate that it represents a new paradigm of signal transduction. This model is pictorially presented, and it may become a prototype for certain other neurosensory processes.

EXPERIMENTAL PROCEDURES

Antibodies. The specificities of antibodies against ONE-GC and GCAP1 have been described previously (*27*, *28*). The antibodies were affinity purified. The PDE2 antibody was purchased from Santa Cruz Biotechnology, Inc. (Santa Cruz, CA). Secondary antibodies conjugated to a fluorescent dye (DyLight 488 and DyLight 549) were purchased from Jackson ImmunoResearch Laboratories, Inc. (West Grove, PA).

GCAPs Knockout Mice. GCAPs knockout ($GCAP1^{-/-}$-$GCAP2^{-/-}$) mice used as the source of the retina and olfactory epithelium were kindly provided by A. Dizhoor (Salus University) with the permission of J. Chen (University of Southern California, Los Angeles, CA).

Immunohistochemistry. Mice were sacrificed by lethal injection of ketamine/xylazine (the protocol approved by the Salus University IUCAC) and perfused through the heart, first with a standard Tris-buffered saline (TBS) and then with freshly prepared 4% paraformaldehyde in TBS. Tissues (MOE and retina) were fixed for 1−4 h in 4% paraformaldehyde with TBS at 4 °C, cryoprotected in 30% sucrose overnight at 4 °C, and cut into 20 μm sections using Hacker-Bright OTF5000 microtome cryostat (HACKER Instruments and Industries Inc., Winnsboro, SC). For ONE-GC or GCAP1 immunostaining, the sections were washed with TBS, blocked in 10% preimmune donkey serum in a TBS/0.5% Triton X-100 mixture (TTBS) for 1 h at room temperature, washed with TTBS, incubated with ONE-GC or GCAP1 antibody (diluted 50:1) in blocking solution overnight at 4 °C, washed with TTBS, incubated with a DyLight 488-conjugated donkey anti-rabbit antibody (200:1) for 1 h, and washed with TTBS. For PDE2A immunostaining, the sections were incubated with 10% goat serum in TTBS, washed with TTBS, incubated with a PDE2A antibody (50:1) in blocking solution for 1 h, washed with TTBS, incubated with a DyLight 549-conjugated goat anti-rabbit antibody (200:1) for 30 min, washed with TTBS, and covered with UltraCruz mounting medium (Santa Cruz Biotechnology, Inc.). Images were acquired using an inverted Olympus IX81 microscope/FV1000 spectral laser confocal system and analyzed using Olympus FluoView FV10-ASW software. Digital images were processed using Adobe Photoshop.

Recombinant YFP-Tagged GCAP1 and CFP-Tagged ONE-GC. The bovine GCAP1 sequence was amplified by PCR from a cDNA clone using a forward primer 5′-TCAGATCTCGAGGCAGCCATGGGGAACATTATGAGCG-3′ and reverse primer 5′-CCCAACAGAATTCGAGAGCCGTCGGCCTCC-3′, thus adding Kozak's motif in front of the ATG translation start codon, mutating the STOP codon, and adding XhoI restriction sites at both ends. The amplified sequence was inserted into the XhoI-digested pZsYellow1-N1 vector (Clontech-TaKaRa Bio Co.) using an "In-fusion" kit (Invitrogen).

CFP-labeled ONE-GC was obtained in a manner identical to that of YFP-labeled GCAP1 except that the PCR-amplified ONE-GC sequence (forward primer 5′-CCGGACTCAAGATCTCGAGGCCACCATGGCAGGTCTGCA-3′ and reverse primer 5′-TCGAAGCTTGAGCTCGAGTGAGCAGACTCTGGCGAGCTTTG-3′) was inserted into the pAmCyan1-N1 vector (Clontech-TaKaRa Bio Co.). For both YFP-GCAP1 and CFP-ONE-GC, proper ligation was verified by sequencing. The resulting constructs were used for transfection of COS cells.

Expression in COS Cells. COS cells were grown in coverslip chambers (two 4 cm^2 chambers per slide) in DMEM medium supplemented with 10% fetal bovine serum and transfected with the GCAP1-YFP and/or ONE-GC-CFP expression constructs using the Ca^{2+} phosphate coprecipitation technique (*29*). Seventy-two hours after transfection, the cells were viewed directly or fixed in 4% paraformaldehyde in Tris-buffered saline (TBS) for 15 min at room temperature.

Preparation of Olfactory Neuroepithelial Membranes Preincubated with Uroguanylin. Mouse MOE was homogenized in 250 mM sucrose/10 mM Tris-HCl (pH 7.4)/1 mM $CaCl_2$ buffer containing protease inhibitors (Sigma-Aldrich). The homogenate was centrifuged at 1000*g*, and the supernatant was incubated on ice for 10 min with 10^{-6} M uroguanylin. Following the incubation, the homogenate was centrifuged at 100000*g* and the pellet (membrane fraction) was washed three times with 50 mM Tris-HCl (pH 7.4)/10 mM $MgCl_2$ buffer; the pellet represented the membrane fraction. Washed membranes were suspended in the same buffer. Control membranes were prepared identically except that the homogenate was incubated without the addition of uroguanylin.

Guanylate Cyclase Activity Assay. Control olfactory neuroepithelial membrane fractions, or fractions preincubated with uroguanylin, were assayed for guanylate cyclase activity as described previously (*25*). Briefly, membranes were incubated on an ice bath with or without GCAP1 in the assay system containing 10 mM theophylline, 15 mM phosphocreatine, 20 μg of creatine kinase, and 50 mM Tris-HCl (pH 7.5), adjusted to a free Ca^{2+} concentration of 10 μM with precalibrated Ca^{2+}/EGTA solutions (Molecular Probes). The total assay volume was 25 μL. The reaction was initiated by addition of the substrate solution (4 mM $MgCl_2$ and 1 mM GTP, final concentrations) and the mixture maintained by incubation at 37 °C for 10 min. The reaction was terminated by the addition of 225 μL of 50 mM sodium acetate buffer (pH 6.2), and then the mixture was heated on a boiling water bath for 3 min. The amount of cyclic GMP formed was determined by a radioimmunoassay (*30*).

Expression of the ONE-GC Fragment of Amino Acids 836−1110 and GCAP1. Expression and purification of the ONE-GC fragment of amino acids 836−1110 were as described previously (*27*), and those of GCAP1 were as described in ref *31*.

SPR Spectroscopy. Sensorgrams were recorded using a BIAcoreX-100 system. For immobilization, the ONE-GC fragment of amino acids 836−1110 was dissolved in 0.05 M sodium acetate buffer (pH 4) and coupled to the CM5 sensor chip. The immobilization level was ~4 ng/mm^2. An independent flow cell on the chip was subjected to a "blank immobilization" (no ONE-GC fragment immobilized) and used as a control

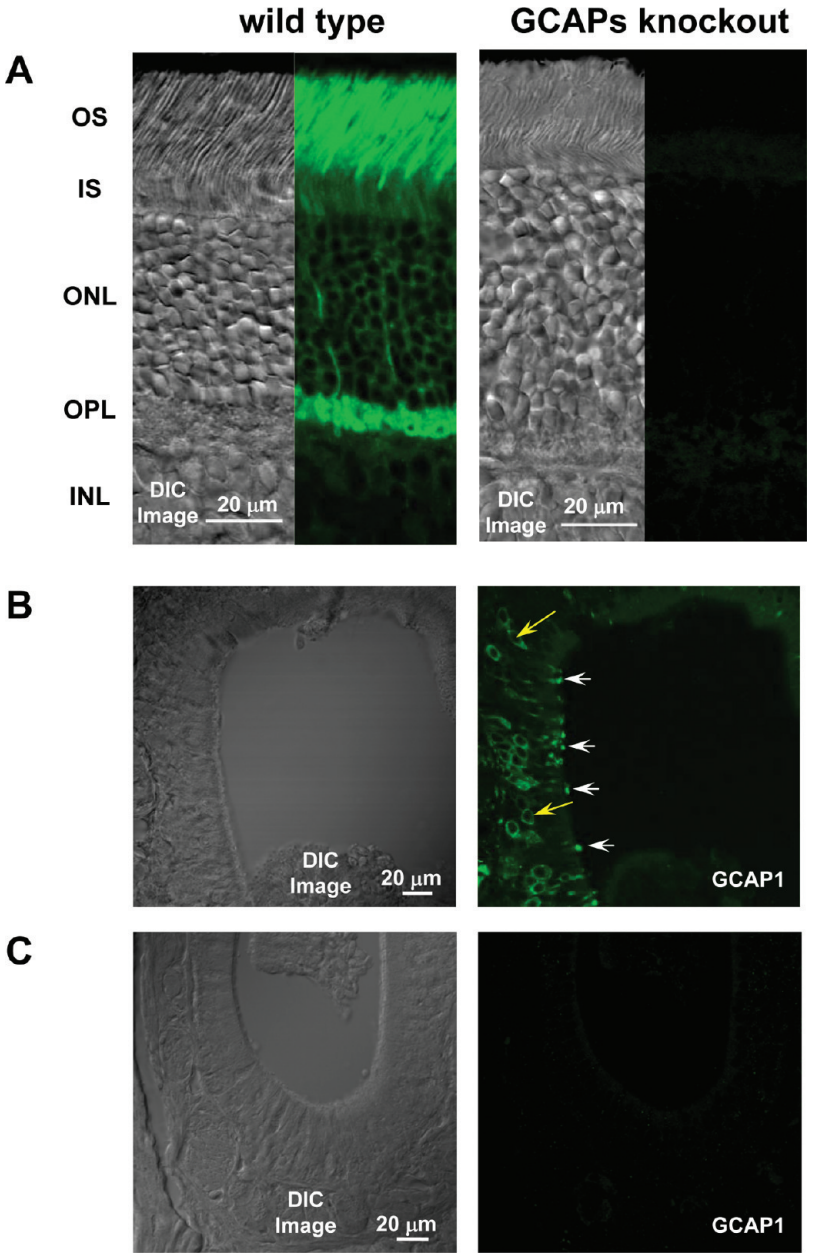

FIGURE 1: Immunoreactivity of GCAP1 in the mouse retina and olfactory neuroepithelium. (A) The affinity-purified antibody was used to immunostain retinal cryosections from the wild type and GCAP1$^{-/-}$GCAP2$^{-/-}$ (GCAPs knockout) mice. For each type of mouse, the left panel presents the differential interference contrast (DIC) image of the section showing the retinal layers (indicated to the left) and the right panels show staining with the GCAP1 antibody. In the retina from the wild-type mouse, the staining is strong in rod and cone outer segments and in the OPL. In the retina from the GCAPs knockout mouse, there is no staining in either retinal layer. The same antibody was used to immunostain cryosections of the olfactory neuroepithelium from the wild-type (B) and GCAPs knockout (C) mice. In panels B and C, the left panels show the DIC images and the right panels immunostaining with the GCAP1 antibody. In the olfactory neuroepithelial section from the wild-type mouse (B), selected olfactory neurons show intense staining with the GCAP1 antibody. The staining is intense in the cilia (four indicated by white arrows) and less intense in the dendrites and somas (two indicated by yellow arrows). The staining is absent in the GCAPs knockout mouse (C).

flow cell. The running buffer contained 10 mM HEPES (pH 7.5), 150 mM NaCl, 20 mM $MgCl_2$, 1 mM $CaCl_2$, and 0.005% surfactant P-20. GCAP1 was dissolved in the running buffer at varying concentrations (from 0.063 to 8 μM) and flushed over both cells. The sensor surface was regenerated after each cycle with 0.05 M glycine (pH 2). Binding was observed as an increase in resonance units (RU) and analyzed via BIAcoreX100.

RESULTS

A Scattered Population of Olfactory Neurons Expresses GCAP1. Rat MOE expresses GCAP1 at the mRNA and protein level (*27*). To identify the regions of MOE in which GCAP1 is expressed, its localization pattern was analyzed by immunostaining. To critically validate the antibody specificity for this approach, GCAP1 immunostaining of the wild-type and the GCAP1/GCAP2 double-knockout (GCAPs knockout) mouse retinas was tested (Figure 1A). Intense GCAP1 immunoreactivity was observed in the wild-type photoreceptor outer segments (Figure 1A, wild type), easily recognized by their typical morphology and location and, as observed previously (*28*), in the OPL regions. In contrast, the corresponding layers in the GCAPs knockout mice retina show no staining (Figure 1A, GCAPs knockout). Thus, the antibody is highly specific for GCAP1

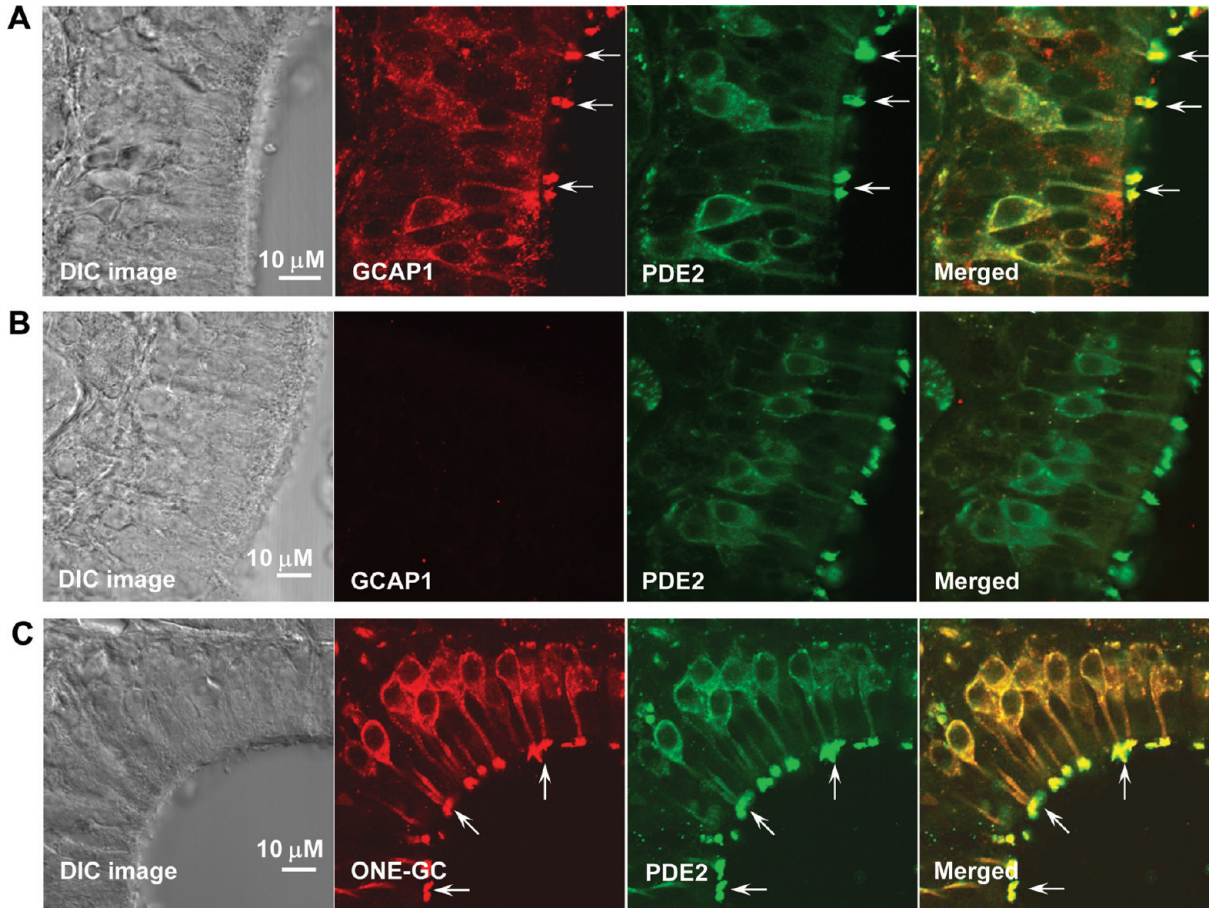

FIGURE 2: GCAP1 is expressed in the same manner as ONE-GC and PDE2A in the olfactory neurons. Cryosections of the olfactory neuroepithelium from the wild-type and GCAPs knockout mice were immunostained with GCAP1 and PDE2A antibodies or ONE-GC and PDE2A antibodies as described in Experimental Procedures. The DIC images showing the integrity of the olfactory neuroepithelium sections are presented at the left (DIC image). (A) A cryosection of the wild-type mouse olfactory neuroepithelium was immunostained with GCAP1 and PDE2A antibodies. Intense staining with either antibody was observed in the cilia (three intense signals are indicated with arrows) and lower-intensity staining in the dendrites and somas. (B) A cryosection of the GCAPs knockout mouse olfactory neuroepithelium was immunostained with GCAP1 and PDE2A antibodies. There was no immunoreactivity with the GCAP1 antibody, whereas intense labeling of selected neurons with the anti-PDE2A antibody was observed. (C) A cryosection of the wild-type mouse olfactory neuroepithelium was immunostained with ONE-GC and PDE2A antibodies. Strong signals with both antibodies were observed in the cilia (three of several signals are indicated with arrows). The dendrites and somas of the immunoreactive neurons were stained as well. The right panels (Merged) present the composite images of GCAP1 and PDE2 or ONE-GC and PDE2 staining and show that both GCAP1 and ONE-GC are coexpressed with PDE2A.

detection and is ideal for screening the presence of GCAP1 in the mouse olfactory epithelium.

GCAP1 immunolabeling was present in the thinly distributed population of the olfactory sensory neurons (Figure 1B, right). The cilia (a few indicated with white arrows) of the neurons were intensely labeled; lower-intensity labeling penetrated into the dendrites and soma (a few indicated with yellow arrows). The GCAPs knockout mice showed a complete absence of staining (Figure 1C, right).

These results establish the presence of GCAP1 in the scattered population of the olfactory sensory neurons. It is predominantly present in the cilia, the site of odorant transduction, yet, in a smaller quantity, is present also in other regions of the olfactory neuron.

GCAP1 and ONE-GC Are Coexpressed with PDE2. The pattern of GCAP1 labeling as shown in Figure 1B is very much like the one established earlier for ONE-GC and cyclic GMP phosphodiesterase PDE2A in mouse and rat olfactory epithelia (*11*, *12*). To assess if GCAP1, ONE-GC, and PDE2A coreside in the ONE-GC neurons of the mouse MOE, double immunostaining was used.

Because antibodies against ONE-GC and GCAP1 used in this study were raised in rabbits, direct double ONE-GC and GCAP1 immunostaining was not feasible. Therefore, this goal was achieved indirectly. Although PDE2A has not been functionally linked with ONE-GC, it always coexists with ONE-GC (*11*). Therefore, the copresence of GCAP1 and PDE2A was determined first and, then, that of ONE-GC and PDE2A, and from them, the copresence of GCAP1 and ONE-GC was assessed.

The GCAP1 panel of Figure 2A shows that the cilia of seven neurons (a few indicated by arrows) in this section exhibit an intense signal (red) generated with the GCAP1 antibody. In most cases, this signal with a lower intensity also continues in the dendrites and somas. The PDE2A panel Figure 2A shows the same section with the green signal generated with the PDE2A antibody. The merged image of the two signals shows that the same neurons express GCAP1 and PDE2A. When the GCAPs knockout mouse MOE was analyzed (Figure 2B), the GCAP1 signal disappeared (Figure 2B, GCAP1) but the PDE2A signal persisted (Figure 2B, PDE2A). These results demonstrate that GCAP1 and PDE2A are coexpressed in the same population of the olfactory sensory neurons and that the absence of GCAP1 expression does not affect the expression of PDE2A.

Consistent with the earlier mouse (*11*) and rat (*12*) MOE studies, this study shows the coexpression of ONE-GC and

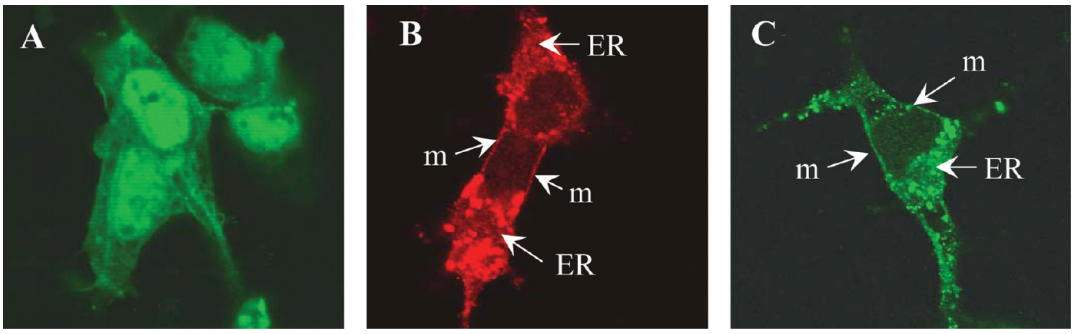

FIGURE 3: Cellular localization of GCAP1 and ONE-GC expressed in COS cells. (A) GCAP1 expressed in COS cells. (B) ONE-GC expressed in COS cells. (C) GCAP1 coexpressed with ONE-GC in COS cells. COS cells were transfected with GCAP1 or/and ONE-GC cDNA. Seventy-two hours after transfection, the cells were fixed with 4% paraformaldehyde and incubated with GCAP1 or ONE-GC antibody followed by incubation with secondary antibodies conjugated with DyLight 488 (green) for GCAP1 immunolocalization and with DyLight 549 (red) for ONE-GC immunolocalization. DyLight 488 was excited at 488 nm and DyLight 549 at 543 nm. The cells were viewed using an inverted Olympus IX81 microscope/FV1000 spectral laser confocal system. Indicated by arrows are the cell membrane (m) and membranes of the endoplasmic reticulum (ER).

PDE2A in the cilia of selected mouse olfactory neurons (in Figure 2C, arrows point to three, of 15, immunostained in this section); the ONE-GC panel shows the red signal generated by the ONE-GC antibody and the PDE2A panel the green signal generated by the PDE2A antibody. When they are merged, the red and green signals overlap completely. Thus, ONE-GC and PDE2A are copresent in selected olfactory neurons.

Because both GCAP1 and ONE-GC are coexpressed with PDE2A, we conclude that GCAP1 is present in the ONE-GC neurons. The presence of ONE-GC, GCAP1, and PDE2A is predominant in the cilia, yet to a lesser degree, they are also present in other regions of the olfactory neurons.

ONE-GC and GCAP1 Physically Interact in the Reconstituted Cell System. On the basis of the results described above that GCAP1 and ONE-GC are physically coupled in the mouse ONE-GC olfactory neurons, it was important to know if this was an intrinsic property of these two molecules or was bestowed upon them through the accessory protein(s) of the olfactory sensory system. In the first situation, wherever these two molecules are copresent in a living cell, they should be bound; in the second, they would be bound exclusively in the olfactory sensory neurons.

This issue was addressed via expression of GCAP1 and ONE-GC individually or together in the heterologous cell system of COS cells and analysis of their cellular localization using the same antibodies that were used for immunolocalization of GCAP1 and ONE-GC in the olfactory epithelium

Expressed alone, GCAP1 was evenly scattered in all cellular compartments, including the nucleus (Figure 3A). An identical pattern of GCAP1 distribution, when expressed alone in HEK cells, was observed previously (*32*). It is consistent with the previous conclusion that although GCAP1 has some ability to bind to the membranes, when expressed alone it behaves as a soluble protein (*32*−*36*). As anticipated, ONE-GC immunoreactivity was localized exclusively to the cellular membranes, the plasma membrane, and the endoplasmic reticulum (ER) (Figure 3B). There was no signal in the nuclear region of the cell.

In the ONE-GC and GCAP1 coexpressing cells, the pattern of GCAP1 immunoreactivity was drastically changed (compare panels A and C of Figure 3). The GCAP1 antibody-generated signal was no longer evenly scattered in all cellular compartments. It was now localized solely to the plasma and ER membranes, the pattern of expression identical to that of ONE-GC. As indicated earlier, the colocalization experiment with GCAP1 and ONE-GC was not possible because of the same source of both antibodies (rabbit). Because GCAP1 coexpressed with ONE-GC follows the pattern of ONE-GC localization, we thereby conclude that the membrane-bound ONE-GC anchors GCAP1 to itself. Thus, it is the intrinsic property of the ONE-GC and GCAP1 to be bound to each other, and no accessory proteins are required for their interaction.

GCAP1 and ONE-GC Are Functionally Interlocked. To assess if the physical colocalization of GCAP1 and ONE-GC advances to their functional interaction, the reconstituted COS cell system was analyzed via FRET. The principle of this technique is that if the distance between two proteins is less than 10 Å (functional interaction distance) an excited donor will transfer its energy to the acceptor, causing it to fluoresce at the expense of the donor's fluorescence. Thus, the acceptor quenches the fluorescence of the donor. One of the most common FRET pairs consists of cyan fluorescent protein (CFP) and yellow fluorescent protein (YFP). The CFP emission spectrum (λ_{max} = 475 nm) overlaps with the YFP absorption spectrum (λ_{max} = 512 nm). Therefore, these two fluorescent proteins were used to tag GCAP1 and ONE-GC. GCAP1 was tagged with YFP and ONE-GC with CFP, and the fusion proteins were expressed in COS cells.

The initial experiments were designed to verify that the fluorescent tag does not affect the expression of the fusion proteins. When GCAP1-YFP was expressed alone in COS cells, the fluorescence was dispersed evenly in the cell (Figure 4A). This pattern of fluorescence distribution remained unchanged in repeated transfections despite varying amounts of GCAP1-YFP cDNA used for transfection and was virtually identical to that obtained via immunocytochemical analysis.

When GCAP1-YFP was coexpressed with ONE-GC in COS cells, the distribution of GCAP1-linked YFP fluorescence changed drastically (Figure 4B). It was now limited to the plasma and ER membranes, following the pattern of ONE-FC expression. We thus conclude that the localization results obtained with immunostaining and intrinsic fluorescence of the fusion proteins are in complete agreement.

On the basis of these conclusions, the fluorescence quenching experiment was performed. The COS cells were cotransfected with GCAP1-YFP and ONE-GC-CFP. CFP was the donor and YFP the acceptor-quencher. The cells were excited at 458 nm (CFP excitation wavelength), and the emitted fluorescence was observed at 480 nm (emission of CFP) and 530 nm (emission of

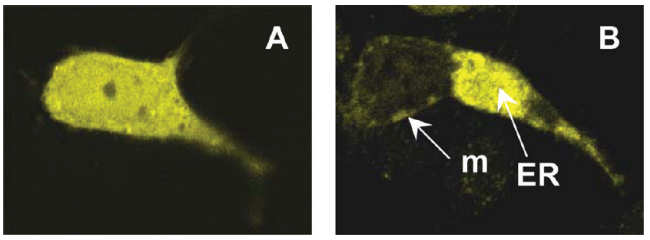

FIGURE 4: Colocalization of GCAP1-YFP with ONE-GC-CFP in live COS cells. (A) GCAP1-YFP was expressed in COS cells. Laser excitation was at 515 nm. The GCAP1-YFP fusion protein is present in the entire cell. (B) GCAP1-YFP was coexpressed with ONE-GC in COS cells. Laser excitation was at 515 nm. In the presence of ONE-GC, fusion protein GCAP1-YFP localizes to cellular membranes, plasma membranes, and ER membranes, the site of ONE-GC expression.

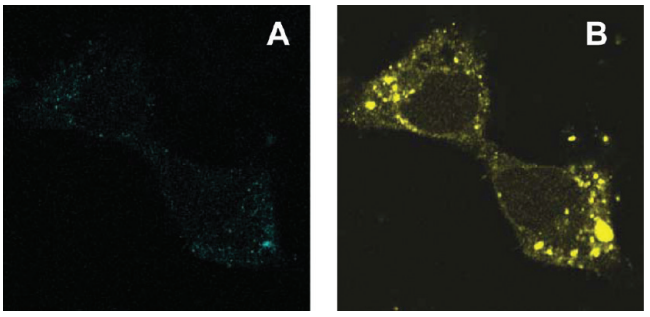

FIGURE 5: Coexpression of GCAP1-YFP with ONE-GC-CFP quenches CFP fluorescence. GCAP1-YFP and ONE-GC-CFP were coexpressed in COS cells. Seventy-two hours after transfection, the cells were observed under a confocal microscope. Laser excitation was at 458 nm, and the emission was observed at 480 nm (CFP) (A) and 530 nm (YFP) (B).

YFP). The results are presented in Figure 5. The presence of GCAP1-YFP together with ONE-GC-CFP resulted in practically nonexisting fluorescence of CFP at 480 nm (Figure 5A) and in significant emission of yellow fluorescence by YFP at 530 nm (Figure 5B). The ability of GCAP1-linked YFP to quench the ONE-GC-linked CFP fluorescence and the fact that the extent of quenching is inversely proportional to the distance between the fluorophore and the quencher show that in a living COS cell ONE-GC and GCAP1 are colocalized within a distance allowing their physical interaction. We therefore conclude that GCAP1 and ONE-GC constitute a physically locked transduction system.

GCAP1 Binds to the Segment of Amino Acids 836−1110 and Stimulates ONE-GC Activity. To define the GCAP1-ONE-GC transduction system in biochemical terms, the site and the binding kinetics of GCAP1 with ONE-GC were assessed through SPR spectroscopy and direct functional analyses.

Previous studies have shown that GCAP1 binds to the fragment of amino acids 836−1110 of ONE-GC (*27*). Therefore, a soluble construct representing this fragment of ONE-GC was expressed in bacteria and purified to homogeneity. The fragment was functionally active, containing intrinsic guanylate cyclase activity of 3 pmol of cyclic GMP min^{-1} (mg of protein)$^{-1}$. It also possessed Ca^{2+}-modulated GCAP1-dependent activity, responding to GCAP1 in a dose-dependent fashion in the presence of a saturating amount of Ca^{2+} (10 μM) (Figure 6A). Thus, this fragment was suitable for the direct binding analyses.

The fragment was immobilized on a sensor chip, and incremental concentrations of GCAP1 were supplied in the mobile phase containing 10 μM Ca^{2+}. A representative set of sensorgrams is presented in Figure 6B. The respective fitting curves, derived after fitting to a 1:1 Langmuir binding model, are also shown. It is evident from Figure 6 that the fitting curves deviate from the experimental data especially in the dissociation phase. Therefore, the binding kinetics was determined graphically. To determine the half-maximal binding (EC_{50}), the experimental RU values were plotted as a function of GCAP1 concentration (Figure 6C). The EC_{50} of GCAP1 was 0.5 μM. Scatchard analysis of the binding data (Figure 6D) resulted in a K_D value of 0.65 μM. This K_D value for binding of GCAP1 to the ONE-GC fragment of amino acids 836−1110 is in agreement with the 0.5 μM EC_{50} value of GCAP1 for the wild-type ONE-GC activation (*27*). The calculated equilibrium association constant, K_A, is 1.5×10^6 M^{-1}. Thus, GCAP1 binds ONE-GC with moderate affinity.

It is of interest to note that these binding kinetics between GCAP1 and ONE-GC are very similar to those of the other Ca^{2+} sensor of ONE-GC, neurocalcin δ (*14*).

GCAP1 Is a Ca^{2+} Sensor of the Odorant-Linked ONE-GC Transduction System in the Olfactory Sensory Neurons. Consistent with the past (*11*, *12*) and our findings that ONE-GC mouse MOE contains the ONE-GC membrane guanylate cyclase transduction system, we assessed whether under the native conditions GCAP1 functions as a Ca^{2+} sensor of ONE-GC. The membrane fraction of the mouse MOE was incubated with incremental concentrations of GCAP1 in the presence of a saturating amount (10 μM) of Ca^{2+} or in its complete absence (1 mM EGTA added to the reaction mixture). In the presence of Ca^{2+}, GCAP1 stimulated the membrane guanylate cyclase activity in a dose-dependent fashion. The half-maximal stimulation was at ~0.5 μM GCAP1, and the maximal stimulation of ~3-fold above the basal value was observed at 2 μM GCAP1 [Figure 7 (●)]. In the absence of Ca^{2+}, GCAP1 was totally ineffective [Figure 7 (○)]. These results demonstrate that like recombinant ONE-GC (Figure 1A in ref *27*), GCAP1 is a natural Ca^{2+} sensor component of ONE-GC.

This conclusion was brought to the physiological level with an identical study conducted in the GCAPs knockout mouse membranes, which lacked GCAP1 and GCAP2. The membrane fractions of the MOE isolated from the wild-type (control) and GCAP1$^{-/-}$GCAP2$^{-/-}$ mice were assayed for guanylate cyclase activity in the presence of 1 mM EGTA (Ca^{2+}-depleted conditions) and 10 μM Ca^{2+}. For the wild-type membranes, the specific activity was ~11 pmol of cyclic GMP min^{-1} (mg of protein)$^{-1}$ in the absence of Ca^{2+} and ~56 pmol of cyclic GMP min^{-1} (mg of protein)$^{-1}$ in the presence of Ca^{2+} (Figure 8A). The difference between these two activities reflects the combined contributions of the Ca^{2+}-dependent modulators of ONE-GC activity in the olfactory neuroepithelium, GCAP1, neurocalcin δ, and hippocalcin (*14*, *26*). To directly assess the contribution of the GCAP1-modulated ONE-GC pathway, the membranes of the GCAP1$^{-/-}$-GCAP2$^{-/-}$ olfactory neuroepithelium were assayed under the same conditions. The specific activity in the absence of Ca^{2+} was identical to that of the wild-type membranes, ~11 pmol of cyclic GMP min^{-1} (mg of protein)$^{-1}$; in the presence of Ca^{2+}, the activity was ~37 pmol of cyclic GMP min^{-1} (mg of protein)$^{-1}$ (Figure 8A). Thus, the input of GCAP1-modulated ONE-GC activity is reflected in the difference between the activity of the wild-type and GCAP1$^{-/-}$-GCAP2$^{-/-}$ neuroepithelial membranes and constitutes approximately 34% of total Ca^{2+}-dependent ONE-GC activity.

This conclusion was validated by the reconstitution experiment. Membranes of the wild-type and GCAPs knockout olfactory neuroepithelium were reconstituted with exogenous GCAP1.

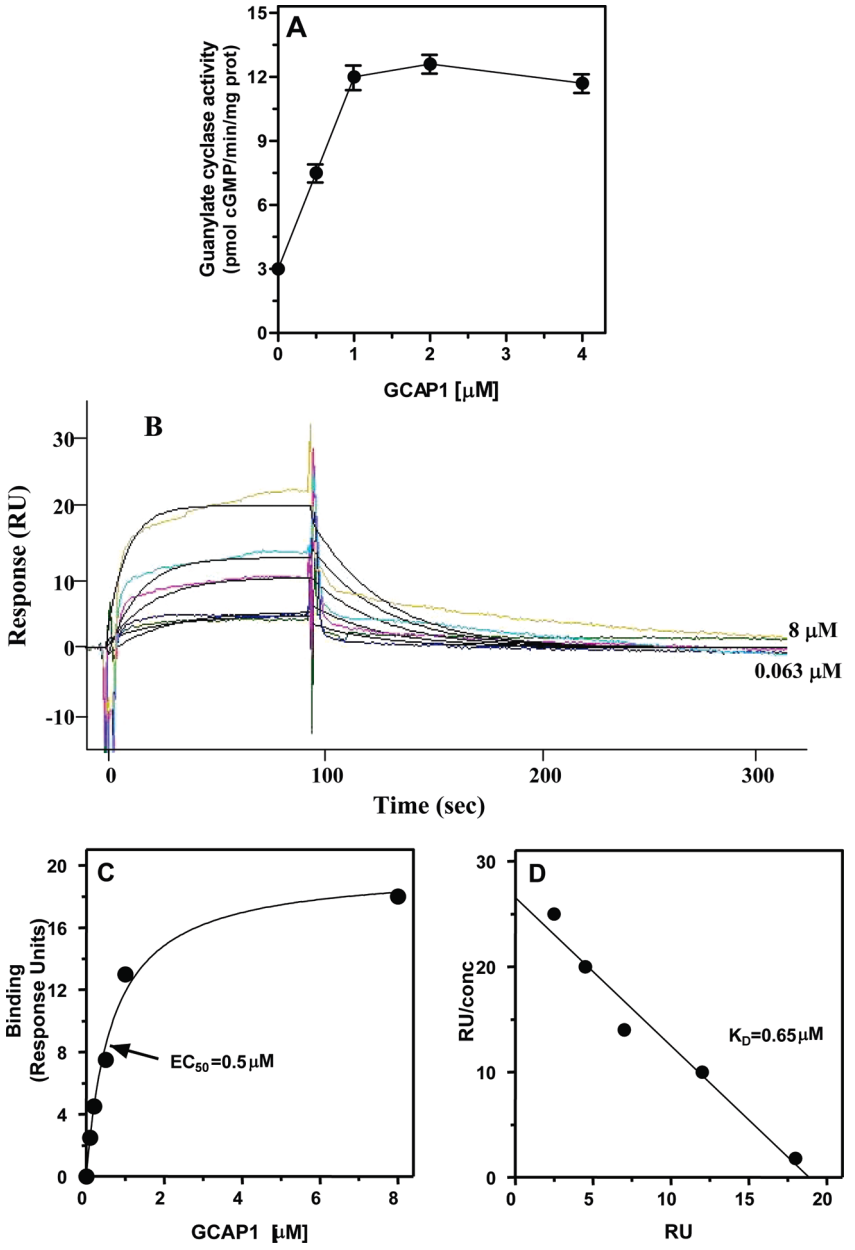

FIGURE 6: Binding of GCAP1 to the ONE-GC fragment of amino acids 836−1110. SPR analysis. (A) The ONE-GC fragment consisting of amino acids 836−1110 was expressed in bacterial cells as a soluble protein as described in Experimental Procedures and analyzed for GCAP1-dependent activity. The experiment was conducted in triplicate and repeated two times with separate preparations of the ONE-GC fragment. The results presented are means ± the standard deviation from these experiments. (B) The ONE-GC fragment of amino acids 836−1110 was immobilized on a CM5 sensor chip, and GCAP1 was supplied in the mobile phase at concentrations between 0.063 and 8 μM in running buffer. A typical set of overlaid sensorgrams together with fitting curves is shown. The curves presented were obtained after subtraction of the effect of buffers and salts on resonance signals using the uncoated (blank) surface in flow cell 1 as the reference surface using BIAevaluation. (C) Binding (RU) as a function of the concentration of GCAP1. (D) Scatchard transformation of the binding data. The experiment was repeated five times with different GCAP1 preparations. The results presented are from one typical experiment.

The rationale for the experiment was that exogenous GCAP1 should bring the cyclase activity to approximately the same maximal level in both types of membranes, and indeed, GCAP1 stimulated guanylate cyclase activity in a dose-dependent manner (Figure 8B). The activity of the wild-type membranes was stimulated ~3-fold above the basal level and that of the $GCAP1^{-/-}GCAP2^{-/-}$ membranes 4-fold, reaching the maximal activity of ~170 of pmol cyclic GMP min^{-1} (mg of protein)$^{-1}$.

We thereby conclude that GCAP1 is the physiological Ca^{2+} sensor of the odorant-linked ONE-GC transduction system.

GCAP1 Is a Ca^{2+} Modulator of the Odorant Uroguanylin Signaling of ONE-GC Activity. The copresence of ONE-GC and GCAP1 in the olfactory cilia strongly suggested that GCAP1 is involved in odorant signal transduction. Because ONE-GC responds to the odorant, uroguanylin, stimulation by activating a two-step, Ca^{2+}-independent and Ca^{2+}-dependent, signaling cascade, it was warranted to analyze if Ca^{2+} sensor GCAP1 is involved in the processing of the Ca^{2+}-dependent step.

Freshly isolated mouse olfactory neuroepithelium was homogenized under Ca^{2+}-depleted conditions (1 mM EGTA). The homogenate was first preincubated with 10^{-6} M uroguanylin, and then the membranes were tested for guanylate cyclase activity in the presence of increasing concentrations of GCAP1 at 10 μM

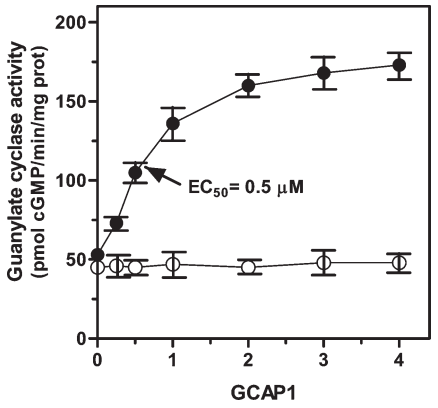

FIGURE 7: Ca^{2+}-dependent activation of ONE-GC by GCAP1. The olfactory neuroepithelium was isolated from wild-type mice and homogenized in 250 mM sucrose/10 mM Tris-HCl (pH 7.5) buffer, and the particulate fraction was isolated. This was analyzed for basal and GCAP1-dependent guanylate cyclase activity in the presence of 10 μM Ca^{2+} (●) or 1 mM EGTA (○). The experiment was conducted in triplicate and repeated three times for the wild-type mouse and two times for the knockout mouse. The results presented are the average ± the standard deviation from these experiments.

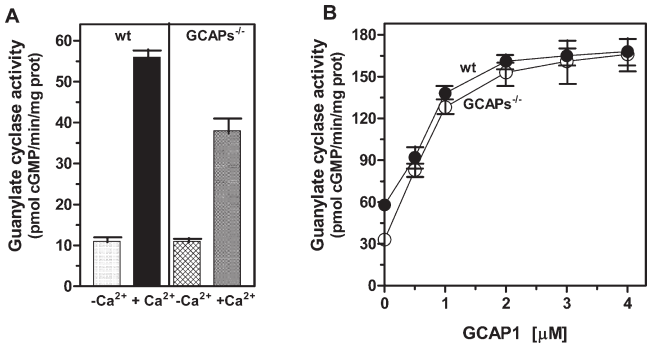

FIGURE 8: GCAP1-modulated ONE-GC system in the olfactory neuroepithelium. (A) Particulate fractions of the olfactory neuroepithelium were isolated from the wild-type (wt) and GCAPs knockout (GCAPs$^{-/-}$) mice. Membranes were assayed for guanylate cyclase activity in the presence of 1 mM EGTA ($-Ca^{2+}$) or 10 μM Ca^{2+} ($+Ca^{2+}$). (B) The membranes were assayed for guanylate cyclase activity in the presence of 10 μM Ca^{2+} and indicated concentrations of GCAP1. The amount of cyclic GMP formed was measured by a radioimmunoassay. The experiment was conducted in triplicate and repeated two times with separate membrane preparations. The results presented (mean ± standard error) are from one experiment.

Ca^{2+}. A control experiment was performed identically, except the homogenate was preincubated, without uroguanylin.

The basal guanylate cyclase activity was 45 pmol of cyclic GMP min^{-1} (mg of protein)$^{-1}$ (Figure 9). In the presence of increasing concentrations of GCAP1, the ONE-GC activity of mock-preincubated membranes increased by ~3.5-fold [Figure 9 (○)]. The picture, however, was different for membranes preincubated with uroguanylin. Here the GCAP1 dose-dependent Ca^{2+} signaling of ONE-GC resulted in a more than 12-fold stimulation of ONE-GC activity, from 45 to 560 pmol of cyclic GMP min^{-1} (mg of protein)$^{-1}$ [Figure 9 (●)]. Thus, the combined effects of uroguanylin and GCAP1 far exceed the sum of their individual effects; they are synergetic.

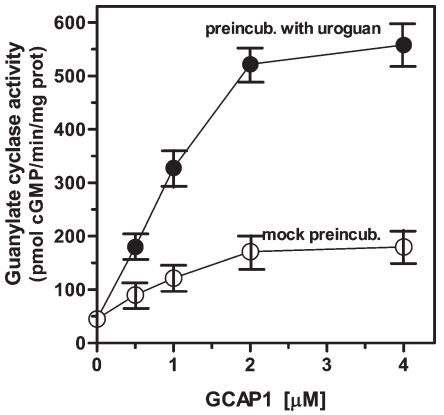

FIGURE 9: Synergetic effect of uroguanylin and GCAP1 on ONE-GC activity. Olfactory neuroepithelium from the wild-type mouse was homogenized in the absence of Ca^{2+} and preincubated with 10^{-6} M uroguanylin, and the membrane fraction was prepared and assayed for guanylate cyclase activity in the presence of 10 μM Ca^{2+} and increasing concentrations of GCAP1. Membranes from mock-preincubated homogenates were treated as controls. The experiment was conducted in triplicate and repeated three times with separate homogenates. The results are means ± the standard deviation from these experiments.

DISCUSSION

In the developing field of mammalian membrane guanylate cyclase, this study is a continuation in exposing its new mechanistic means of signal transduction. The study documents that (1) GCAP1 is a constitutive part of the odorant-linked ONE-GC transduction machinery, (2) it is its Ca^{2+} sensor component, (3) it functions in a fashion that is the opposite of that in phototransduction, and (4) the odorant−ONE-GC-GCAP1 transduction system operates through a two-step signaling mechanism.

GCAP1, a Constitutive Part of the Odorant-Linked ONE-GC Transduction Machinery. To date, GCAP1 is considered exclusively the Ca^{2+}-sensor component of the phototransduction system. Its functions are to capture the incremental (nanomolar to semimicromolar) Ca^{2+} signals and inhibit ROS-GC1 activity and the production of cyclic GMP, the second messenger of the light signal (*37*−*41*). With this mode in the rod and cone outer segments, it modulates the recovery and adaption processes of phototransduction. In the identical mode, it functions in the cone pedicles (*28*), olfactory bulb neurons (*42*), pinealocytes (*43*), and spermatogenic cells of the testes (*44*).

These findings demonstrate that in the mouse olfactory cilia (1) GCAP1 is a physiological constituent of the ONE-GC signaling pathway (thus, it is not solely a constituent of the phototransduction system), (2) the GCAP1/ONE-GC transduction pathway neither is connected nor overlaps with the major cyclic AMP signaling pathway, and (3) besides PDE2A (*11*) and CNGA3 (*12*), GCAP1 is also a marker protein of the ONE-GC neurons.

GCAP1 Is the Positive Ca^{2+} Sensor Modulator of the ONE-GC. Like in the in vitro reconstitution and the rat olfactory neuroepithelium systems (*27*), in the mouse MOE GCAP1 stimulates ONE-GC activity in the presence of Ca^{2+}. Thus, its *modi operandi* in the phototransduction and odorant transduction processes are in opposite fashions, as are the consequences. The first *modus operandus* causes a decline in the production of cyclic GMP. This, closure of the cyclic GMP-gated channels and continuous extrusion of Ca^{2+} through its exchanger cause hyperpolarization in the outer segments. The second mode causes acceleration of cyclic GMP production and depolarization of the olfactory ciliary membranes (*45*).

(*i*) *How Does GCAP1 Exhibit Reversible Operation of Structural Homologues ROS-GC1 and ONE-GC?* This riddle, as yet, has not been solved. This study, however, discloses

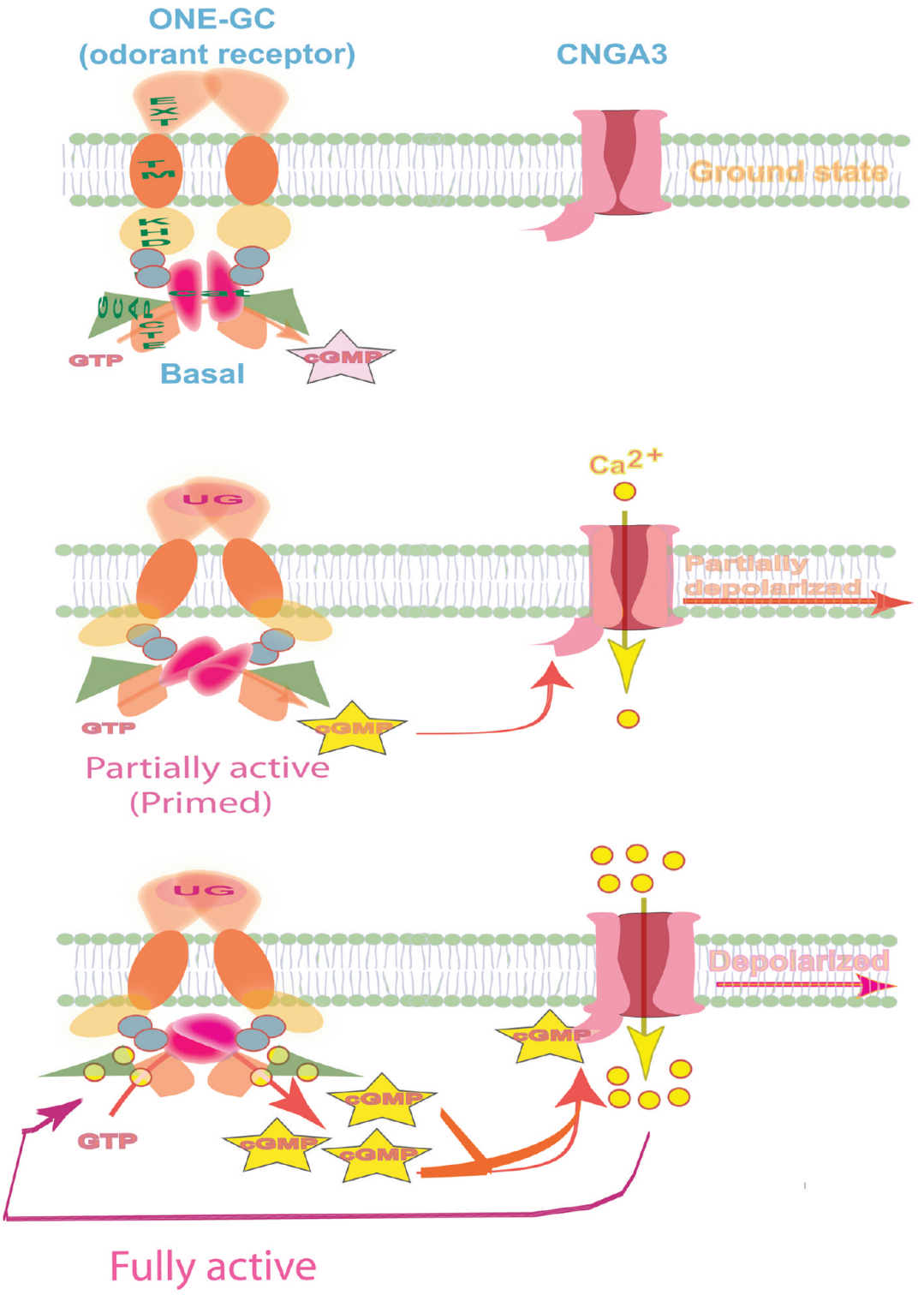

FIGURE 10: Two-step uroguanylin-GCAP1-ONE-GC signal transduction model in the olfactory receptor neuron. The Model. Basal indicates the ground state. The $[Ca^{2+}]_i$ in the resting cilia is 60−100 nM; the ONE-GC dimer is bound to GCAP1, and its activity is in the basal state. For the primed, partially active state, odorant, uroguanylin, signaling begins when it binds to the extracellular receptor domain of ONE-GC. In a Ca^{2+}-independent fashion, it causes structural changes in the domain, which are transduced to the intracellular domain and finally to the catalytic module, causing its partial ~3-fold activation. The small amount of cyclic GMP produced as a result of this activation opens a fraction of the CNGA3 channels and some influx of Ca^{2+}, which partially depolarizes the ONE-GC neuron's membrane. For the fully active state, the Ca^{2+} ions that entered the ONE-GC neuron as a result of the partial ONE-GC activation bind to GCAP1 and create two physiological consequences: (1) full activation of ONE-GC, and (2) the resulting cyclic GMP opens the maximal number of CNGA3 channels, causing maximal influx of Ca^{2+} and depolarization of the ONE-GC neuron's membrane.

two clues. (1) The signal transduction sites of GCAP1 in these two cyclases are different. In ROS-GC1, it resides in two short regions of its juxtamembrane domain, M445−L456 and L503−I522 (*46*); in ONE-GC, it is in the C-terminal domain, residues 836−1110 (*27*), (2) In phototransduction-linked ROS-GC1, initiation of the GCAP mode is indirect, via the light signal-induced cascade occurring through G-protein, transducin; in ONE-GC, it is direct, originating and being transmitted through ONE-GC.

GCAP1 Is Bound to ONE-GC in the Native Olfactory Sensory Neurons. Previous immunoprecipitation results demonstrate an important olfactory-relevant feature of GCAP1. It is the fact that GCAP1 is permanently bound to ONE-GC in the olfactory neurons (*27*). Thus, only changes in free $[Ca^{2+}]_i$ but not the GCAP1-ONE-GC association−dissociation cycle define the velocity of the odorant-linked ONE-GC transduction machinery. This is identical to phototransduction where GCAP1 is permanently bound to ROS-GC (reviewed in ref *47*).

Consistent with its role as a physiological partner to the ONE-GC odorant transduction system, SPR studies show that it binds ONE-GC with moderate affinity (K_D = 0.67 μM; K_A = 1.5×10^6 M^{-1}).

(*i*) *Gene Deletion and Rescue Operations Demonstrate That GCAP1 Contributes ~34% to the ONE-GC Signal Transduction System*. We can now conclude that three Ca^{2+} sensors define ONE-GC modulation; they are neurocalcin δ, Hpca, and GCAP1, and their respective contributions to ONE-GC modulation are 27% for neurocalcin δ (*26*), 30% for hippocalcin (*26*), and 34% for GCAP1.

GCAP1-Modulated Odorant Signal Transduction Model. The evidence presented here demonstrates that the GCAP1-modulated uroguanylin signaling of ONE-GC activity is a two-step process. As shown previously (*25*) and also now, the first process occurs at the ONE-GC extracellular domain by its interaction with the odorant. This step is Ca^{2+}-independent. It primes ONE-GC, partially (~3-fold) activates it, and prepares it for the second GCAP1- and Ca^{2+}-dependent step, which causes full activation of the guanylate cyclase, 4-fold over the primed step, overall ~12-fold. This signal transduction mechanism is pictorially presented in Figure 10.

In the formulation of this model, the following features of ONE-GC are considered general, derived from other members of the membrane guanylate cyclase family. (1) ONE-GC is a homodimer (*48*). (2) Its contact points for homodimerization reside in its extracellular and catalytic domains (*48*−*50*). (3) The monomers of the catalytic domains are antiparallel (*48*, *49*).

Model. For the basal state, the $[Ca^{2+}]_i$ in the resting cilia is 60−100 nM (*1*); the ONE-GC dimer is bound to Ca^{2+}-free GCAP1, and its activity is in the basal state. For the primed, partially active state, odorant, uroguanylin, signaling begins when it binds to the extracellular receptor domain of ONE-GC (*20*). In a Ca^{2+}-independent fashion, it causes structural changes, which are successively transduced to the catalytic module, causing its partial ~3-fold activation. The small amount of cyclic GMP produced as a result of this activation opens a fraction of the CNGA3 channels and some influx of Ca^{2+}, which partially depolarizes the ONE-GC neuron's membrane. For the fully active state, the Ca^{2+} ions that entered the ONE-GC neuron as a result of partial ONE-GC activation bind to GCAP1. Ca^{2+}-bound GCAP1 causes full activation of ONE-GC; cyclic GMP formed opens the maximal number of CNGA3 channels, causing the maximal influx of Ca^{2+} and depolarization of the ONE-GC neuron's membrane.

CONCLUSION

Besides disclosing an intriguing GCAP1-modulated odorant transduction mechanism, this study has begun to answer a seminal question related to the general role of cyclic GMP signaling pathway in odorant signaling. How can a single membrane guanylate cyclase transduce multiple forms of the odorant?

The emerging answer is that it is defined by the architecture of the odorant receptor guanylate cyclase. Consider ONE-GC. It is a transducer of three odorants: green pepper (*14*, *21*), uroguanylin (*19*, *20*, *25*), and atmospheric CO_2 (*23*, *24*). Studies with the last two odorants reveal that these odorants achieve specificity of ONE-GC signaling through their divergent mechanisms by which they modulate their specific domains in ONE-GC (*25*). The chemosensory odorant, uroguanylin, starting from the extracellular domain of ONE-GC requires multiple signal transduction events, which are Ca^{2+}-independent and Ca^{2+}-dependent (*25*), but bicarbonate, the second messenger of CO_2, directly, in a Ca^{2+}-independent fashion binds to the catalytic module of ONE-GC and activates it (*25*). Consistent with our findings and previous findings, uroguanylin signaling at the extracellular receptor domain can switch on at least three Ca^{2+}-dependent transduction pathways, through GCAP1, neurocalcin δ, and hippocalcin. Although, as yet, we do not understand the meaning of these multiple signaling pathways, it is clear that, in contrast to the indirect canonical cyclic AMP-linked pathway, the ONE-GC transduction pathway is extremely flexible and with its multiple control devices is capable of being the common transducer of the divergent odorant signals.

REFERENCES

1. Munger, S. D., Leinders-Zufall, T., and Zufall, F. (2009) Subsystem organization of the mammalian sense of smell. *Annu. Rev. Physiol. 71*, 115–140.
2. Nakamura, T. (2000) Cellular and molecular constituents of olfactory sensation in vertebrates. *Comp. Biochem. Physiol., Part A: Mol. Integr. Physiol. 126*, 17–32.
3. Menini, A. (1999) Calcium signaling and regulation in olfactory neurons. *Curr. Opin. Neurobiol. 9*, 419–426.
4. Schild, D., and Restrepo, D. (1998) Transduction mechanisms in vertebrate olfactory receptor cells. *Physiol. Rev. 78*, 429–466.
5. Belluscio, L., Gold, G. H., Nemes, A., and Axel, R. (1998) Mice deficient in G(olf) are anosmic. *Neuron 20*, 69–81.
6. Breer, H. (2003) Olfactory receptors: Molecular basis for recognition and discrimination of odors. *Anal. Bioanal. Chem. 37*, 427–433.
7. Buck, L. B. (1995) Unraveling chemosensory diversity. *Cell 83*, 349–352.
8. Buck, L. B. (2000) The molecular architecture of odor and pheromone sensing in mammals. *Cell 100*, 611–618.
9. Lai, P. C., Singer, M. S., and Crasto, C. J. (2005) Structural activation pathways from dynamic olfactory receptor-odorant interactions. *Chem. Senses 30*, 781–792.
10. Fülle, H. J., Vassar, R., Foster, D. C., Yang, R. B., Axel, R., and Garbers, D. L. (1995) A receptor guanylyl cyclase expressed specifically in olfactory sensory neurons. *Proc. Natl. Acad. Sci. U.S.A. 92*, 3571–3575.
11. Juilfs, D. M., Fülle, H. J., Zhao, A. Z., Houslay, M. D., Garbers, D. L., and Beavo, J. A. (1997) A subset of olfactory neurons that selectively express cGMP-stimulated phosphodiesterase (PDE2) and guanylyl cyclase-D define a unique olfactory signal transduction pathway. *Proc. Natl. Acad. Sci. U.S.A. 94*, 3388–3395.
12. Meyer, M. R., Angele, A., Kremmer, E., Kaupp, U. B., and Muller, F. (2000) A cGMP-signaling pathway in a subset of olfactory sensory neurons. *Proc. Natl. Acad. Sci. U.S.A. 97*, 10595–10600.
13. Duda, T., Jankowska, A., Venkataraman, V., Nagele, R. G., and Sharma, R. K. (2001) A novel calcium-regulated membrane guanylate cyclase transduction system in the olfactory neuroepithelium. *Biochemistry 40*, 12067–12077.
14. Duda, T., Fik-Rymarkiewicz, E., Venkataraman, V., Krishnan, A., and Sharma, R. K. (2004) Calcium-modulated ciliary membrane guanylate cyclase transduction machinery: Constitution and operational principles. *Mol. Cell. Biochem. 267*, 107–122.
15. Zufall, F., and Munger, S. D. (2010) Receptor guanylyl cyclases in mammalian olfactory function. *Mol. Cell. Biochem. 334*, 191–197.
16. Duda, T., Venkataraman, V., and Sharma, R. K. (2007) Constitution and operational principles of the retinal and odorant-linked neurocalcin δ-dependent Ca^{2+} modulated ROS-GC transduction machinery. In Neuronal Calcium Sensor Proteins (Philippov, P., and Koch, K.-W., Eds.) pp 91−113, Nova Science Publishers, Inc., Hauppauge, NY.

17. Sharma, R. K., and Duda, T. (2010) Odorant-linked ROS-GC subfamily membrane guanylate cyclase transduction system. *Mol. Cell. Biochem. 334*, 181–189.
18. Duda, T., and Sharma, R. K. (2010) Distinct ONE-GC transduction modes and motifs of the odorants: Uroguanylin and CO_2. *Biochem. Biophys. Res. Commun. 391*, 1379–1384.
19. Leinders-Zufall, T., Cockerham, R. E., Michalakis, S., Biel, M., Garbers, D. L., Reed, R. R., Zufall, F., and Munger, S. D. (2007) Contribution of the receptor guanylyl cyclase GC-D to chemosensory function in the olfactory epithelium. *Proc. Natl. Acad. Sci. U.S.A. 104*, 14507–14512.
20. Duda, T., and Sharma, R. K. (2008) ONE-GC membrane guanylate cyclase, a trimodal odorant signal transducer. *Biochem. Biophys. Res. Commun. 367*, 440–445.
21. Moon, C., Jaberi, P., Otto-Bruc, A., Baehr, W., Palczewski, K., and Ronnett, G. V. (1998) Calcium-sensitive particulate guanylyl cyclase as a modulator of cAMP in olfactory receptor neurons. *J. Neurosci. 18*, 3195–3205.
22. Paul, A. K., Marala, R. B., Jaiswal, R. K., and Sharma, R. K. (1987) Coexistence of guanylate cyclase and atrial natriuretic factor receptor in a 180-kD protein. *Science 235*, 1224–1226.
23. Hu, J., Zhong, C., Ding, C., Chi, Q., Walz, A., Mombaerts, P., Matsunami, H., and Luo, M. (2007) Detection of near-atmospheric concentrations of CO_2 by an olfactory subsystem in the mouse. *Science 317*, 953–957.
24. Sun, L., Wang, H., Hu, J., Han, J., Matsunami, H., and Luo, M. (2009) Guanylyl cyclase-D in the olfactory CO_2 neurons is activated by bicarbonate. *Proc. Natl. Acad. Sci. U.S.A. 106*, 2041–2046.
25. Duda, T., and Sharma, R. K. (2009) Ca^{2+}-modulated ONE-GC odorant signal transduction. *FEBS Lett. 583*, 1327–1330.
26. Krishnan, A., Duda, T., Pertzev, A., Kobayashi, M., Takamatsu, K., and Sharma, R. K. (2009) Hippocalcin, new Ca^{2+} sensor of a ROS-GC subfamily member, ONE-GC, membrane guanylate cyclase transduction system. *Mol. Cell. Biochem. 325*, 1–14.
27. Duda, T., Krishnan, R., and Sharma, R. K. (2006) GCAP1: Antithetical calcium sensor of ROS-GC transduction machinery. *Calcium Binding Proteins 1*, 102–107.
28. Venkataraman, V., Duda, T., Vardi, N., Koch, K. W., and Sharma, R. K. (2003) Calcium-modulated guanylate cyclase transduction machinery in the photoreceptor−bipolar synaptic region. *Biochemistry 42*, 5640–5648.
29. Sambrook, M. J., Fritsch, E. F., and Maniatis, T. (1989) Molecular Cloning: A Laboratory Manual, 2nd ed., Cold Spring Harbor Laboratory Press, Plainview, NY.
30. Nambi, P., Aiyar, N. V., and Sharma, R. K. (1982) Adrenocorticotropin-dependent particulate guanylate cyclase in rat adrenal and adrenocortical carcinoma: Comparison of its properties with soluble guanylate cyclase and its relationship with ACTH-induced steroidogenesis. *Arch. Biochem. Biophys. 217*, 638–646.
31. Duda, T., Venkataraman, V., Jankowska, A., Lange, C., Koch, K. W., and Sharma, R. K. (2000) Impairment of the rod outer segment membrane guanylate cyclase dimerization in a cone-rod dystrophy results in defective calcium signaling. *Biochemistry 39*, 12522–12533.
32. Peshenko, I. V., Olshevskaya, E. V., and Dizhoor, A. M. (2008) Binding of guanylyl cyclase activating protein 1 (GCAP1) to retinal guanylyl cyclase (RetGC1). The role of individual EF-hands. *J. Biol. Chem. 283*, 21747–21757.
33. Otto-Bruc, A., Buczylko, J., Surgucheva, I., Subbaraya, I., Rudnicka-Nawrot, M., Crabb, J. W., Arendt, A., Hargrave, P. A., Baehr, W., and Palczewski, K. (1997) Functional reconstitution of photoreceptor guanylate cyclase with native and mutant forms of guanylate cyclase-activating protein 1. *Biochemistry 36*, 4295–4302.
34. Olshevskaya, E. V., Hughes, R. E., Hurley, J. B., and Dizhoor, A. M. (1997) Calcium binding, but not a calcium-myristoyl switch, controls the ability of guanylyl cyclase-activating protein GCAP-2 to regulate photoreceptor guanylyl cyclase. *J. Biol. Chem. 272*, 14327–14333.
35. Hwang, J. Y., and Koch, K. W. (2002) Calcium- and myristoyl-dependent properties of guanylate cyclase-activating protein-1 and protein-2. *Biochemistry 41*, 13021–13028.
36. Vogel, A., Schröder, T., Lange, C., and Huster, D. (2007) Characterization of the myristoyl lipid modification of membrane-bound GCAP-2 by ^2H solid-state NMR spectroscopy. *Biochim. Biophys. Acta 1768*, 3171–3181.
37. Nicol, G. D., and Miller, W. H. (1978) Cyclic GMP injected into retinal rod outer segments increases latency and amplitude of response to illumination. *Proc. Natl. Acad. Sci. U.S.A. 75*, 5217–5220.
38. Nicol, G. D., and Miller, W. H. (1979) Evidence that cyclic GMP regulates membrane potential in rod photoreceptors. *Nature 280*, 64–66.
39. Miller, W. H. (1982) Physiological evidence that light-mediated decrease in cyclic GMP is an intermediary process in retinal rod transduction. *J. Gen. Physiol. 80*, 103–123.
40. Rätscho, N., Scholten, A., and Koch, K. W. (2010) Diversity of sensory guanylate cyclases in teleost fishes. *Mol. Cell. Biochem. 334*, 207–214.
41. Koch, K. W., Duda, T., and Sharma, R. K. (2010) Ca^{2+}-modulated vision-linked ROS-GC guanylate cyclase transduction machinery. *Mol. Cell. Biochem. 334*, 105–115.
42. Duda, T., Venkataraman, V., Krishnan, A., Nagele, R. G., and Sharma, R. K. (2001) Negatively calcium-modulated membrane guanylate cyclase signaling system in the rat olfactory bulb. *Biochemistry 40*, 4654–4662.
43. Venkataraman, V., Nagele, R., Duda, T., and Sharma, R. K. (2000) Rod outer segment membrane guanylate cyclase type 1-linked stimulatory and inhibitory calcium signaling systems in the pineal gland: Biochemical, molecular, and immunohistochemical evidence. *Biochemistry 39*, 6042–6052.
44. Jankowska, A., Burczynska, B., Duda, T., Warchol, J. B., and Sharma, R. K. (2007) Calcium-modulated rod outer segment membrane guanylate cyclase type 1 transduction machinery in the testes. *J. Androl. 28*, 50–58.
45. Sharma, R. K., and Duda, T. (2006) Calcium sensor neurocalcin δ-modulated ROS-GC transduction machinery in the retinal and olfactory neurons. *Calcium Binding Proteins 1*, 7–11.
46. Lange, C., Duda, T., Beyermann, M., Sharma, R. K., and Koch, K.-W. (1999) Regions in vertebrate photoreceptor guanylyl cyclase ROS-GC1 involved in Ca^{2+}-dependent regulation by guanylyl cyclase-activating protein GCAP-1. *FEBS Lett. 460*, 27–31.
47. Koch, K. W. (2006) GCAPs, the classical neuronal calcium sensors in the retina: A Ca^{2+}-relay model of guanylate cyclase activation. *Calcium Binding Proteins 1*, 3–6.
48. Venkataraman, V., Duda, T., Ravichandran, S., and Sharma, R. K. (2008) Neurocalcin δ Modulation of ROS-GC1, a New Model of Ca^{2+} Signaling. *Biochemistry 47*, 6590–6601.
49. Liu, Y., Ruoho, A. E., Rao, V. D., and Hurley, J. H. (1997) Catalytic mechanism of the adenylyl and guanylyl cyclases: Modeling and mutational analysis. *Proc. Natl. Acad. Sci. U.S.A. 94*, 13414–13419.
50. Ogawa, H., Qiu, Y., Ogata, C. M., and Misono, K. S. (2004) Crystal structure of hormone-bound atrial natriuretic peptide receptor extracellular domain: Rotation mechanism for transmembrane signal transduction. *J. Biol. Chem. 279*, 28625–28631.